Effects of Contact Structure on the Transient Evolution of HIV Virulence

Sang Woo Park[1] Benjamin M. Bolker[1,2,3,*]

1 Department of Mathematics & Statistics, McMaster University, Hamilton, Ontario, Canada
2 Department of Biology, McMaster University, Hamilton, Ontario, Canada
3 Institute for Infectious Disease Research, McMaster University, Hamilton, Ontario, Canada

* bolker@mcmaster.ca

Abstract

Early in an epidemic, high densities of susceptible hosts select for relatively high parasite virulence; later in the epidemic, lower susceptible densities select for lower virulence. Thus over the course of a typical epidemic the average virulence of parasite strains increases initially, peaks partway through the epidemic, then declines again. However, precise quantitative outcomes, such as the peak virulence reached and its timing, may depend sensitively on epidemiological details. Fraser *et al.* proposed a model for the eco-evolutionary dynamics of HIV that incorporates the tradeoffs between transmission and virulence (mediated by set-point viral load, SPVL) and their heritability between hosts. Their models use implicit equations to capture the effects of partnership dynamics that are at the core of epidemics of sexually transmitted diseases. Our models combine HIV virulence tradeoffs with a range of contact models, modeling partnership formation and dissolution and allowing for individuals to transmit disease outside of partnerships. We assess summary statistics such as the peak virulence (corresponding to the minimum expected time of progression to AIDS) across models for a range of parameters applicable to the HIV epidemic in sub-Saharan Africa. Although

virulence trajectories are broadly similar across models, the timing and magnitude of the virulence peak vary considerably. Previously developed implicit models predicted lower virulence and slower progression at the peak (a minimum of 15 years to progress to AIDS) compared both to more realistic models and to simple random-mixing models with no partnership structure at all (both with a minimum of ≈ 7.25 years to progress to AIDS). In this range of models, the simplest random-mixing structure best approximates the most realistic model; this surprising outcome occurs because the dominance of extra-pair contact in the realistic model swamps the effects of partnership structure.

Author Summary

Pathogens such as HIV can evolve rapidly when the environment changes. Such changes include decreases in the probability that an infectious contact (such as a sneeze for a respiratory disease, or an unprotected sex act for a sexually transmitted disease) encounters an uninfected, susceptible person and thus has a chance to transmit the pathogen. Disease spread during an epidemic reduces the fraction of susceptible people in the population and thus changes the direction of parasite evolution. While researchers have explored these evolutionary dynamics with simulations, their models have neglected important processes such as people entering and leaving sexual partnerships. We compared several evolutionary models that include partnership dynamics and sexual contact outside of stable partnerships. Models of intermediate complexity predicted lower virulence over the course of the epidemic (a minimum of 15 years to progress to AIDS) than either more realistic models or simple models without any partnership structure at all (both approx. 7.25 years to progress to AIDS), because sexual contact outside of stable partnerships tended to wash out the effects of contact structure. The large effect of epidemiological details on evolutionary dynamics suggests that researchers trying to predict the evolution of pathogens should proceed with caution.

Introduction

The evolution of pathogen virulence has both theoretical and, potentially, practical importance. In general, evolutionary theory suggests that pathogens with higher reproduction numbers ($\mathcal{R}_0$) — that is, the number of secondary infections caused by a single infected host over the course of its infectious period — will tend to increase in prevalence relative to strains with lower reproductive ratios. Pathogens can increase their reproduction numbers either by increasing their transmission rate, the rate (per infected host) at which they infect new hosts, or by decreasing their clearance or disease-induced mortality rate, the rate at which hosts recover or die from disease. The *trade-off theory* [1] postulates that transmission and disease-induced mortality rates are both driven by the rate at which the pathogen exploits host resources for within-host reproduction, and that pathogen evolution will thus strike a balance between the pathogen's rate of transmission to new hosts and its rate of killing its host (or of provoking the host's immune system to eliminate it). Some biologists have criticized the tradeoff theory [2,3], but others have successfully applied it to a variety of host-pathogen systems [4–7].

Fraser *et al.* have applied these ideas to HIV, showing that the virus appears to satisfy the prerequisites of the tradeoff theory. The *set-point viral load* (SPVL: i.e., the characteristic virus load measured in blood during the intermediate stage of infection) is a measurable proxy for the rate of HIV within-host reproduction. Higher viral loads are correlated with shorter progression times (higher virulence). Studies of discordant couples — stable sexual partnerships with one infected and one uninfected partner — have shown that SPVL is (1) correlated with faster transmission (the time to infection of the uninfected partner is shorter when their partner has a higher SPVL) and (2) heritable (when the uninfected member of the couple does become infected, their SPVL is similar to their partner's). Furthermore, the rate of transmission increases with increasing SPVL (and hence with decreasing progression time) but with a decreasing slope as progression time decreases, fulfilling the requirements of the tradeoff theory [8]. Subsequent studies [10–12] used these data to parameterize mechanistic models of HIV virulence evolution, suggesting that HIV invading a novel population would initially evolve increased virulence, peaking after approximately 100-200 years and then

declining slightly to a long-stable virulence level. 32

The work of Shirreff *et al.* [10], and particularly the predicted transient peak in HIV 33
virulence midway through the epidemic, highlights the importance of interactions 34
between epidemiological and evolutionary factors [13,14]. However, despite these 35
studies' attention to detail at the individual or physiological level, the contact structures 36
used in these models are relatively simple. 37

As we discuss in detail below, existing models of HIV eco-evolutionary dynamics 38
either use implicit models that incorporate the average effects of within-couple sexual 39
contact — without representing the explicit dynamics of pair formation and dissolution 40
or accounting for extra-partnership contact — or use an agent-based formulation with 41
parameters that effectively lead to random mixing among infected and uninfected 42
individuals. Here we explore the effects of incorporating *explicit* contact structure in 43
eco-evolutionary models. 44

Because our main goal is to explore how conclusions about virulence evolution 45
depend on the way in which contact structure is modeled, we consider a series of models 46
with increasing levels of complexity in the contact structure, but simplify some of the 47
other epidemiological processes (such as the within-host life history of HIV). We 48
evaluate our models across a wide range of parameters, using a Latin hypercube design; 49
for each model run, we compute a set of metrics that summarize the evolutionary 50
trajectory of SPVL over the course of the epidemic. 51

Materials and Methods 52

Infection dynamics 53

As in Shirreff *et al.* [10], our models explicitly track the evolution of mean $\log_{10}$ SPVL 54
(which we denote as α), rather than the rate of progression to AIDS itself (hereafter 55
"virulence" will refer either to the SPVL, or to the rate of progression to AIDS; these 56
two quantities are deterministically linked in the model). In contrast to Shirreff *et al.*, 57
we use a single-stage disease model instead of accounting explicitly for progression 58
through the three main stages of HIV infection (primary, asymptomatic, and disease), 59
and we use an exponentially distributed infectious period instead of a more realistic 60

Weibull-distributed infectious period; we show below that our results are not overly sensitive to this simplification. We account for varying transmission rates and durations of each disease stage by summing the durations of three stages (again based on Shirreff *et al.*'s model) and taking the duration-weighted average of transmission rates of three stages. Thus the within-couple transmission rate, β, for our models is given by:

$$\beta(\alpha) = \frac{D_P\beta_P + D_A(\alpha)\beta_A(\alpha) + D_D\beta_D}{D_P + D_A(\alpha) + D_D},\tag{1}$$

where the duration of infection (D_P and D_D) and rate of transmission (β_P and β_D) of the Primary and Disease stages of infection are independent of the host's SPVL (Table 1 gives definitions, units, and values for all parameters). . Following Shirreff *et al.*, the duration of infection (D_A) and rate of transmission (β_A) for the Asymptomatic stage are Hill functions of the SPVL:

$$\begin{aligned} D_A(\alpha) &= \frac{D_{\max}D_{50}^{D_k}}{V_\alpha^{D_k} + D_{50}^{D_k}},\\ \beta_A(\alpha) &= \frac{\beta_{\max}V_\alpha^{\beta_k}}{V_\alpha^{\beta_k} + \beta_{50}^{\beta_k}}, \end{aligned}\tag{2}$$

where $V_\alpha = 10^\alpha$.

The uncoupled and extra-couple transmission rates (i.e., the rates of transmission among people outside of a stable partnership, or between people inside of a stable partnership and people other than their partner) are scaled by multiplying the within-couple transmission rate β by the contact ratios c_u/c_w and c_e/c_w (see Appendix S1). Simplifying the model of HIV pathogenesis from three stages to a single stage could affect our conclusions about the evolution of virulence (e.g. Kretzschmar and Dietz [17] show that pair formation dynamics and multiple stages of infectivity have interactive effects on $\mathcal{R}_0$). However, our simplified model produces results that are qualitatively similar to those of Shirreff *et al.*'s [10] model; when our model is calibrated to have a similar initial epidemic growth rate r, the peak $\log_{10}$ SPVL occurs at the same time (≈ 200 years) but slightly higher (4.6 $\log_{10}$ SPVL vs. 4.3 $\log_{10}$ SPVL: Fig 1).

Table 1. Parameter ranges/values. Parameters with fixed values are kept constant throughout simulations while other parameter values are taken from Latin hypercube samples using ranges specified in the table. Values of c and ρ are doubled from those given by Champredon *et al.* because we keep track of individuals in the model, while they keep track of couples. Starred (*) parameters (used in Fig 1), and descriptions of Hill function coefficients, are taken from [10].

Notation	Description	Range/Value	Source
ρ	Partnership formation rate	1/10-2/5 per year	[15]
c	Partnership dissolution rate	1/15-1/5 (1.25*) per year	[15]
c_u/c_w	Relative contact rate for uncoupled transmission	1/5-5	Assumption
c_e/c_w	Relative contact rate extra-couple	0.01-1	[15]
β_P	Rate of transmission during primary infection	1.31-5.09 (2.76*) per year	[18]
β_D	Rate of transmission during high transmission disease stage	0.413-1.28 (0.76*) per year	[18]
D_P	Duration of primary infection	1.23/12-6/12 (0.25*) years	[18]
D_D	Duration of high transmission disease stage	4.81/12-14/12 (0.75*) years	[18]
$\beta_{\max}$	Maximum rate of transmission during asymptomatic stage	0.317 per year	[10]
β_{50}	SPVL at which infectiousness is half maximum	13938 copies per ml	[10]
β_k	Hill coefficient: steepness of increase in infectiousness as a function of SPVL	1.02	[10]
$D_{\max}$	Duration of primary infection	25.4 years	[10]
D_{50}	SPVL at which duration of asymptomatic infection is half maximum	3058 copies per ml	[10]
D_k	Hill coefficient: steepness of decrease in duration as a function of SPVL	0.41	[10]
σ_M	Mutation standard deviation of $\log_{10}$ SPVL	0.12	[10]
$\alpha_{\min}$	Minimum $\log_{10}$ SPVL	2	[10]
$\alpha_{\max}$	Maximum $\log_{10}$ SPVL	7	[10]
n	Number of strains	21 (51*)	Assumption
μ	Mean number of non-cohabiting sexual partners	0.103 - 1.206	[19]
κ	Squared coefficient of variation of number of non-cohabiting sexual partners	0.01 - 100	Assumption

Mutation

Like Shirreff *et al.* [10] we incorporate a between-host mutation process in the SPVL.

We simplify Shirreff *et al.*'s evolutionary model by using a one-to-one

genotype-phenotype mapping rather than allowing for variation in phenotypes of a

single genotype. The mutational process in our model is directly taken from Shirreff *et*
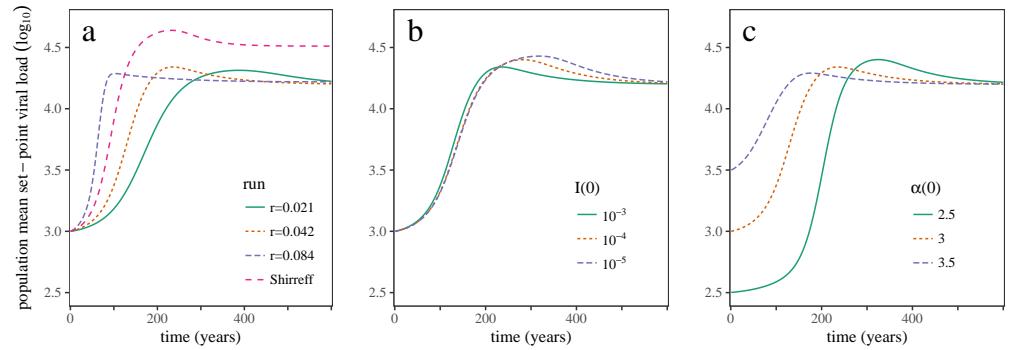
Fig 1. Baseline dynamics. Time series of mean population $\log_{10}$ SPVL using baseline parameters. Each initial condition was varied independently in order to test their effects on transient dynamics of virulence evolution. Note that the initial condition has negligible effect on equilibrium virulence. (a) Contrast between the three-stage Shirreff model and the single-stage model calibrated to varying initial exponential growth rates, r. achieved quicker. (b) Effects of varying initial infectious density $I(0)$. (c) Effects of varying initial mean virulence $\alpha(0)$. The $r = 0.042$ (orange, dotted) curve in panel (a), calibrated to match the epidemic dynamics of Shirreff *et al.*'s model [10], shows that our simplified model can produce similar virulence trajectories. Although virulence dynamics are sensitive to initial conditions, we are still able to achieve similar qualitative dynamics dynamics across a range of parameters. For fair comparison, we hold them constant throughout our simulations.

al.. Over the course of infection, mutation occurs within the host. However, it is assumed that SPVL of the strain transmitted by an infected individual is determined by the SPVL at the time of infection and is not further affected by within-host mutation. Instead, the mutational effect takes place in a single step at the time of transmission. First, the distribution of $\log_{10}$ SPVL is discretized into a vector:

$$\alpha_i = \alpha_{\min} + (\alpha_{\max} - \alpha_{\min})\frac{i-1}{n-1} \qquad i = 1, 2, 3, \ldots n. \tag{3}$$

We have experimented with varying degrees of discretization in the strain distribution (i.e., values of n); in our model runs comparing results with Shirreff *et al.* [10] (Fig 1) we use $n = 51$ (i.e. a bin width of 0.1 $\log_{10}$ SPVL for α), but reducing n to 21 (bin width = 0.25 $\log_{10}$ SPVL) makes little difference; we use this coarser grid for all other simulations reported.

We construct an n by n mutational matrix, M — which is multiplied with the transmission term — so that M_{ij} is the probability that a newly infected individual will have $\log_{10}$ SPVL of α_j given that the infector has $\log_{10}$ SPVL of α_i. Finally, the

probabilities are normalized so that each row sums to 1:   101

$$M_{ij} = \frac{\Phi(\alpha_j + d/2; i) - \Phi(\alpha_j - d/2; i)}{\Phi(\alpha_{\max} + d/2; i) - \Phi(\alpha_{\min} - d/2; i)}, \tag{4}$$

where $\Phi(x; i)$ is the Gaussian cumulative distribution function with mean α_i and   102

variance of σ_M^2, and $d = (\alpha_{\max} - \alpha_{\min})/(n-1)$. Transmission rate and disease induced   103

mortality rates are discretized as well: 104

$$\begin{aligned} \beta_i &= \beta(\alpha_i), \\ \lambda_i &= \frac{1}{D_P + D_A(\alpha_i) + D_D}. \end{aligned} \tag{5}$$

Contact structure and partnership dynamics   105

We developed seven multi-strain evolutionary models covering a gamut including   106

Champredon *et al.*'s relatively realistic [15] and Shirreff *et al.*'s relatively simple [10]   107

contact structures, each of which is based on different assumptions regarding contact   108

structure and partnership dynamics. Specifically, we focus on the effects of the   109

assumptions of (1) instantaneous vs. non-instantaneous partnership formation; (2) zero   110

vs. positive extra-partnership sexual contact and transmission; and (3) homogeneous vs.   111

heterogeneous levels of sexual activity on the evolution of mean $\log_{10}$ SPVL.   112

Our first four models consider explicit partnership dynamics and are based on   113

Champredon *et al.*'s model [15]. The first two ("pair-formation" or "pairform" for short)   114

assume non-instantaneous partnership formation (i.e. individuals spend some time   115

uncoupled, outside of partnerships) and consist of five states that are classified by   116

infection status and partnership status. S is the number of single (uncoupled)   117

susceptible individuals, and I is the number of single infected individuals. SS is the   118

number of concordant negative (susceptible-susceptible) couples, SI is the number of   119

serodiscordant (susceptible-infected) couples, and II is the number of concordant   120

positive (infected-infected) couples. The first ("pairform+epc") includes   121

extra-partnership contact (with both uncoupled individuals and individuals in other   122

partnerships) whereas the second ("pairform") only considers within-couple   123

transmission.   124

The next two models, which are intended to bridge the gap between models with   125

fully explicit pair-formation dynamics and the simpler, implicit models used by Shirreff 126
et al. [10], assume instantaneous partnership formation ("instswitch"). The 127
compartmental structure thus omits the single states S and I, comprising only the three 128
partnered states: SS, SI, and II. Like the first two models, this pair of models differs 129
in their inclusion of extra-pair contact: the third model ("instswitch+epc") includes 130
extra-partnership contact (now only with individuals in other partnerships, since 131
uncoupled individuals do not exist in this model) while the fourth ("instswitch") only 132
considers within-couple transmission. Although these models can also be implemented 133
by setting the partnership formation rate of the explicit partnership models to a high 134
value (and we have tested that both methods in fact produce same results), we model 135
instantaneous partnership formation models independently in order to avoid scaling of 136
partnership formation rate during model calibration affecting the virulence trajectory. 137

The fifth and sixth models represent extreme simplifications of sexual partnership 138
dynamics. One ("implicit") is an implicit serial monogamy model based on the 139
epidemiological model used by Shirreff *et al.* [10]. It is actually a random mixing model 140
that explicitly tracks only the total number of susceptible and infected individuals. 141
However, to reflect the effect of partnership structure, it uses an adjusted transmission 142
rate derived from an approximation of the basic reproduction number of a serial 143
monogamy model with instantaneous pair formation [18]. The second model of this pair 144
("random") is a simple random-mixing model. 145

Lastly, we add a model of heterogeneity in sexual activity to the pairform+epc 146
model ("hetero"). Individuals are divided into different risk groups based on the sexual 147
activity level; we scale all aspects of sexual activity, assuming that sexual activity level 148
in both within- and extra-couple contacts is directly proportional to number of 149
non-cohabiting (extra-couple and uncoupled) partners per year [19] (see Appendix S1). 150
We assume random activity-weighted mixing between risk groups [20]. While this model 151
lacks some important elements, such as age-structured mixing patterns, needed for 152
realistic models of HIV transmission in sub-Saharan Africa, it represents a first step 153
toward assessing the effects of epidemiological complexity. As even the models shown 154
here push the limits of compartmental-based models (the heterogeneity model comprises 155
24530 coupled ordinary differential equations), adding further complexity will probably 156
require a shift to an agent-based model framework, as well as considerable effort in 157

model calibration [11, 21]. 158

The pairform+epc and heterogeneous models use the basic epidemiological 159
framework of Champredon *et al.* [15]. Individuals in single compartment acquire a 160
partner at a rate ρ, and partnerships dissolve at a rate c. Infected individuals in a 161
discordant partnership infect their susceptible partner at a rate β (within-couple 162
transmission rate) and susceptible individuals outside the partnership at a rate c_e 163
(extra-couple transmission rate). Likewise, a single infected individual can infect any 164
susceptible individuals at a rate c_u through uncoupled mixing. Extra-couple and 165
uncoupled transmission are modeled in the same way as in Champredon *et al.*'s model. 166
All the details have been adapted to a multi-strain scenario, so that we track (for 167
example) a matrix II_{ij} that records the number of concordant, HIV-positive couples in 168
which the two partners have $\log_{10}$ SPVL of α_i and α_j. The second through fourth 169
models (pairform, instswitch+epc, instswitch) are derived from the base model by 170
simplifying epidemiological processes (partnership formation and 171
uncoupled/extra-couple contact: see Appendix S1). 172

Latin hypercube sampling 173

Despite considerable effort [15, 18], the parameters determining the rate and structure of 174
sexual partnership change and contact are still very uncertain; this led Champredon *et* 175
al. [15] to adopt a Latin hypercube sampling (LHS) strategy [22] that evaluates model 176
outcomes over a range of parameter values. In order to make sure that our comparisons 177
among models apply across the entire space of reasonable parameter values, and in 178
order to evaluate the differential sensitivity of different model structures to parameter 179
values, we follow a similar protocol and perform LHS over a parameter set including 180
both the early- and late-stage transmission and duration parameters (β_P, D_P, β_D, D_D) 181
and contact/partnership parameters (ρ, c, c_u/c_w, and c_e/c_w). For the heterogeneity 182
model, the mean and squared coefficient of variation (CV) for the number of 183
non-cohabiting partners are sampled as well. We do not allow for uncertainties in 184
parameters that are directly related to the evolutionary process ($\beta_{\max}$, β_{50}, β_k, $D_{\max}$, 185
D_{50}, D_k, σ_M), instead using Shirreff *et al.*'s point estimates throughout [10]. 186

Latin hypercube sampling is done as in Champredon *et al.* [15]. For each parameter, 187

z, its range is divided into $N = 1000$ equal intervals on a log scale: $\qquad$ 188

$$z_i = \exp\left(\log(z_{\min}) + [\log(z_{\max}) - \log(z_{\min})]\frac{i-1}{N-1}\right) \qquad i = 1, 2, 3, \ldots, N. \quad (6)$$

Random permutations of these vectors form columns in a sample parameter matrix; $\qquad$ 189

each row contains a different parameter set that is used for one simulation run. $\qquad$ 190

Table 1 gives the ranges of the model parameters used for LHS. Parameter ranges $\qquad$ 191

regarding contact and partnership dynamics (ρ, c, and c_e/c_w) are taken from $\qquad$ 192

Champredon *et al.* [15], whereas those regarding infection (β_P, D_P, β_D, and D_D) are $\qquad$ 193

taken from Hollingsworth *et al.* [18]. The remaining parameters are taken from Shirreff $\qquad$ 194

et al. [10]. $\qquad$ 195

One parameter in our model, the ratio of uncoupled to within-couple transmission $\qquad$ 196

c_u/c_w, is needed to more flexibly contrast uncoupled and extra-couple transmission $\qquad$ 197

dynamics within multi-strain models (see Appendix S1); it appears neither in either $\qquad$ 198

Shirreff *et al.* nor Champredon *et al.*'s models, so we need to pick a reasonable range for $\qquad$ 199

it. Champredon *et al.* [15] assume that the effective within-couple contact rate and $\qquad$ 200

effective uncoupled contact rate have the same range of 0.05 - 0.25. Given Champredon $\qquad$ 201

et al.'s parameter range, the possible maximum and minimum values of c_u/c_w are 5 and $\qquad$ 202

1/5. Therefore, we use 1/5-5 as the range for the parameter c_u/c_w. Although this adds $\qquad$ 203

more uncertainty to the parameter c_u — Champredon *et al.*'s range implies a 5-fold $\qquad$ 204

difference whereas ours gives a 25-fold difference — we consider the wider range $\qquad$ 205

appropriate, as little is not much known about the uncoupled transmission rate. $\qquad$ 206

Two parameters, mean and the squared coefficient of variation (CV) of number of $\qquad$ 207

non-cohabiting partners, are sampled for heterogeneity in sexual activity. To allow for a $\qquad$ 208

wide range of uncertainty, range for the mean number of non-cohabiting partners was $\qquad$ 209

taken from unmarried men, as that was the group with the largest variability [19]. $\qquad$ 210

Omori *et al.* [19] give a very wide range for the coefficient of variation ($\approx$ 0 - 20, $\qquad$ 211

corresponding to squared CV range of 0-400): we narrowed this range for CV^2 to $\qquad$ 212

0.01-100. At the bottom end of the range, estimating that a group behaves perfectly $\qquad$ 213

homogeneously ($CV = 0$) is likely to be a sampling artifact; at the upper end, the $\qquad$ 214

estimate is also likely to be noisy because of the low mean value among married females $\qquad$ 215

(who have the largest range of CV). We assume that the number of non-cohabiting $\qquad$ 216

partners follows a Gamma distribution.   217

Simulation runs   218

One of the most difficult parts of model comparison is finding parameter sets that are   219
commensurate with many different model structures. For the most part, our models are   220
too complex to easily derive analytical correspondences among them. Given a numerical   221
criterion, such as r (initial exponential growth rate) or $\mathcal{R}_0$ (intrinsic reproductive   222
number), we can adjust one or more parameters by brute force to ensure that all of the   223
models match according to that criterion. While $\mathcal{R}_0$ is often considered the most   224
fundamental property of an epidemic, and might thus seem to be a natural matching   225
criterion, here we focus on matching the initial growth rate r for several reasons. First,   226
our primary interest is in the transient evolutionary dynamics of virulence, which are   227
more strongly affected by r than $\mathcal{R}_0$. Second, r is more directly observable in real   228
epidemics; r can be estimated by fitting an exponential curve to the initial incidence or   229
prevalence curves [23], while $\mathcal{R}_0$ typically requires either (1) knowledge of *all* epidemic 230
parameters or (2) calculations based on r and knowledge of the serial interval or   231
generation interval of the disease [24]. Thus, we scale parameters so that every run has   232
the same initial exponential growth rate in disease incidence.   233

In order to allow for all models to have equal initial exponential growth rate, r, we   234
need to pick a parameter, s, such that $\lim_{s \to 0} r(s) = 0$ and $\lim_{s \to \infty} r(s) = \infty$. As 235
adjusting either partnership change rate (i.e. partnership formation and dissolution   236
rate) or transmission rate fails this requirement for some of our models, we scaled   237
partnership change rate and dissolution rate by the same factor of γ: $\beta_{\mathrm{adj}} = \gamma \beta_{\mathrm{base}}$, 238
$c_{\mathrm{adj}} = \gamma c_{\mathrm{base}}$, $\rho_{\mathrm{adj}} = \gamma \rho_{\mathrm{base}}$. Since transmission rate is adjusted by the scale of γ, 239
uncoupled and extra-couple transmission rates are adjusted as well. For the   240
instantaneous-switching and implicit models, none of which track single individuals,   241
only the transmission rate and partnership dissolution rate (in this case equivalent to   242
the partnership change rate) are adjusted.   243

We run each model for each of 1000 parameter sets chosen by Latin hypercube   244
sampling, with fixed starting conditions of mean $\log_{10}$ SPVL of 3 and epidemic size of   245
10^{-4}. After each run, initial exponential growth rate is calculated. Then, parameters   246

are scaled so that the initial exponential growth rate is scaled to 0.04, a value that   247

approximates the growth rates of Shirreff *et al.*'s original models. For calibration   248

purposes, we run each model for only 500 years (full simulations are run for 4000 years),   249

which is always long enough to capture the exponential growth phase of the model. We   250

use a 4/5 order Runge-Kutta method (`ode45` from the `deSolve` package [25]) for all   251

simulations. (For the heterogeneous model, approximately 10% of the samples failed   252

due to numerical instability.)   253

Although each disease strain's core characteristic is its SPVL, the SPVL has   254

one-to-one correspondences (based on eq. 2) with both the expected time to progression   255

to AIDS and with the rate (probability per unit time) of HIV transmission. Because the   256

time to progression (measured in years) is easier to interpret than SPVL (measured in   257

$\log_{10}$ SPVL units), we summarize the virulence trajectories for each model run in terms   258

of time to progression rather than SPVL. Because the time to progression is inversely   259

related to SPVL (increasing SPVL decreases the time to progression), the time to   260

progression is technically measuring inverse virulence rather than virulence (we did not   261

think that reporting virulence as the rate of progression to AIDS, in units of years^{-1},   262

would help interpretability). For each model we derive the following summary statistics: 263

minimum expected time to progression; time at which this minimum occurs   264

(corresponding to peak virulence — this is also the time at which the maximum rate of   265

progression, maximum SPVL, and maximum transmission rate occur); equilibrium time   266

to progression; and the ratio of progression time at its minimum to the equilibrium   267

value. Equilibrium progression time is calculated after 4000 years of simulated time.   268

Although most simulations reach equilibrium much earlier, we set our time horizon at a   269

much later date as some simulation runs have slow rate of evolution depending on the   270

parameter set and model assumptions.   271

Knowing the minimum progression time, timing of the minimum progression   272

time/peak virulence, and equilibrium progression time provide sufficient detail to   273

identify the overall shape of the virulence trajectory. In particular, knowing the timing   274

of the peak virulence (how many years into the epidemic the virulence peaks) can help   275

epidemiologists guess whether the virulence of an emerging pathogen is likely (1) to   276

have peaked early, possibly even before the pathogen is detected spreading in the   277

population, and decline over the remaining course of the epidemic; (2) to increase, peak,   278

and decline over the foreseeable future; or (3) to increase very slowly, peaking only in $\quad$ 279

the far future. To the extent that our simplistic model for HIV reflects reality, we would $\quad$ 280

take the peak time of 150-300 years (Fig 1c) to mean that, in the absence of treatment, $\quad$ 281

the epidemic would probably still be increasing in virulence. $\quad$ 282

Results $\hfill$ 283

Our simplifications of Shirreff *et al.*'s model [10] reproduce its qualitative behaviour — $\quad$ 284

in particular, its predictions of virulence dynamics — reasonably well. As r decreases $\quad$ 285

from 0.084 to 0.42 (the latter value matching the initial rate of increase in prevalence in $\quad$ 286

Shirreff *et al.*'s full model) the initial trajectory of increasing virulence brackets the rate $\quad$ 287

from the original model (Fig 1a). However, our model produces lower peak virulence $\quad$ 288

(≈ 4.3 vs. ≈ 4.6 $\log_{10}$ SPVL) and equilibrium virulence (≈ 4.25 vs. ≈ 4.5 $\log_{10}$ SPVL) $\quad$ 289

than Shirreff's, even for matching initial incidence trajectories (i.e., $r = 0.042$ year^{-1}). $\quad$ 290

$\qquad$ Changing the initial infectious density ($I(0)$), while it produces the expected changes $\quad$ 291

in the initial epidemic trajectory (Supplementary material), has little effect on the $\quad$ 292

virulence trajectory, making the virulence peaks slightly later and larger as $I(0)$ $\quad$ 293

decreases. Decreasing $I(0)$ allows a longer epidemic phase before the transition to $\quad$ 294

endemic dynamics (Fig 1b). Decreasing the initial virulence also leads to progressively $\quad$ 295

later, larger peaks in virulence (Fig 1c). $\quad$ 296

$\qquad$ Across the entire range of parameters covered by the LHS analysis, all of the classes $\quad$ 297

of models we considered produce qualitatively similar virulence trajectories, which we $\quad$ 298

quantify in terms of the expected time of progression to AIDS (Fig 2: lower progression $\quad$ 299

time corresponds to higher virulence). Although the speed of virulence evolution varies, $\quad$ 300

leading to wide variation in the minimum expected progression time (means ranging $\quad$ 301

from approximately 6 to 12 years), virulence peaks in all models between 200 and 300 $\quad$ 302

years. $\quad$ 303

$\qquad$ Our chosen summary statistics (peak time, minimum expected progression time, $\quad$ 304

equilibrium expected progression time, and relative progression time) all vary $\quad$ 305

considerably across models (Fig 3). We first consider the models of intermediate realism: $\quad$ 306

implicit, instantaneous-switching with and without extra-pair contact, and pair $\quad$ 307

formation without extra-pair contact. Some parameter sets for these models lead to low $\quad$ 308
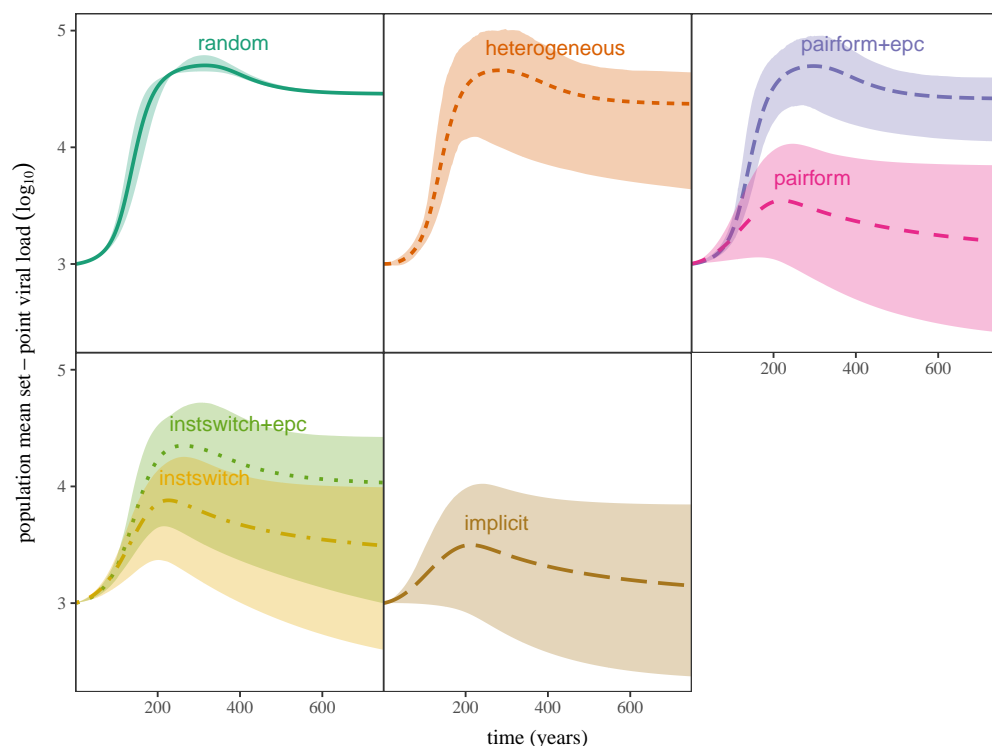
Fig 2. Envelopes of virulence trajectories (population mean $\log_{10}$ SPVL) under all models. All models were run until $t = 4000$ years using parameters from 1000 Latin hypercube samples to illustrate the range of dynamics each model can exhibit. Envelopes contain mid 95% trajectories, while lines within the envelopes show mean trajectories. Truncated series (up to year 800) are shown here.

equilibrium virulence (≈ 18 years to progression); these same sets lead to correspondingly low peak virulence (16 years to progression) and early peak times (before 200 years: Fig 4). At the opposite extreme, parameter sets that produce high equilibrium virulence (8 years to progression) also produce late peaks (> 200 years) and high peak virulence (4 years to progression). The pair-formation without extra-pair contact and implicit models occasionally have parameter sets that select for such low virulence across the board that they never exceed their initial virulence, leading to a tail of peak times near zero.

The most striking aspect of the univariate comparisons in Fig 3, (and the bivariate comparisons in Fig 4) is the similarity between the results of the least (random mixing) and the most complex (pair formation with extra-pair contact, pairform+epc with heterogeneity) models. The random-mixing model has the lowest variability, because it is unaffected by uncertainty in pair formation and extra-pair contact parameters, but
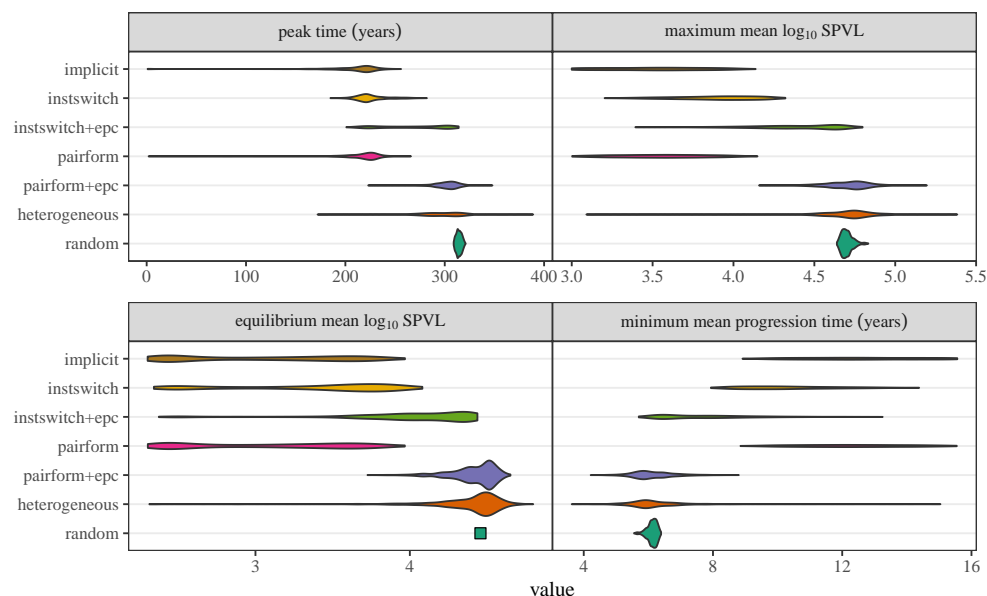
Fig 3. Univariate distributions of summary statistics. For every simulation, three summary statistics were obtained: peak time, maximum mean $\log_{10}$ SPVL, and equilibrium mean $\log_{10}$ SPVL. Peak time is the time at which a virulence trajectory achieves its maximum value (maximum mean $\log_{10}$ SPVL). Equilibrium mean $\log_{10}$ SPVL is taken by taking the mean $\log_{10}$ SPVL value at $t = 4000$. Minimum mean progression time is obtained by applying the hill function to maximum mean $\log_{10}$ SPVL of each run. The distribution of equilibrium mean $\log_{10}$ SPVL (lower left panel) for the random mixing model is very narrow, and has been replaced by a point in order to preserve the vertical axis scaling.

otherwise the virulence dynamics of these three extreme models are remarkably similar. This phenomenon is driven by the strong effects of extra-pair contact in the model with explicit pair formation and extra-pair contact ("pairform+epc" in Figs 2-5). When individuals spend time uncoupled between partnerships, and when these single individuals can transmit disease to coupled individuals, the resulting unstructured mixing overwhelms the effect of structured mixing within couples, leading to mixing that is effectively close to random. Once unstructured mixing is strong, adding realistic heterogeneity of mixing to the model has little effect other than increasing the variability in the outcomes.

These differences are practically as well as scientifically important. The random-mixing, pairform+epc, and heterogeneous models all predict rapid progression to AIDS at the virulence peak (median/95% CI = 6.1 (5.7-6.3), 6.02 (5.04-7.7), 6.03 (4.8-9.2)). In contrast, the implicit model predicts minimum progression times about twice as long: 12.5 (9.6-15.6) years. The corresponding differences in within-couple
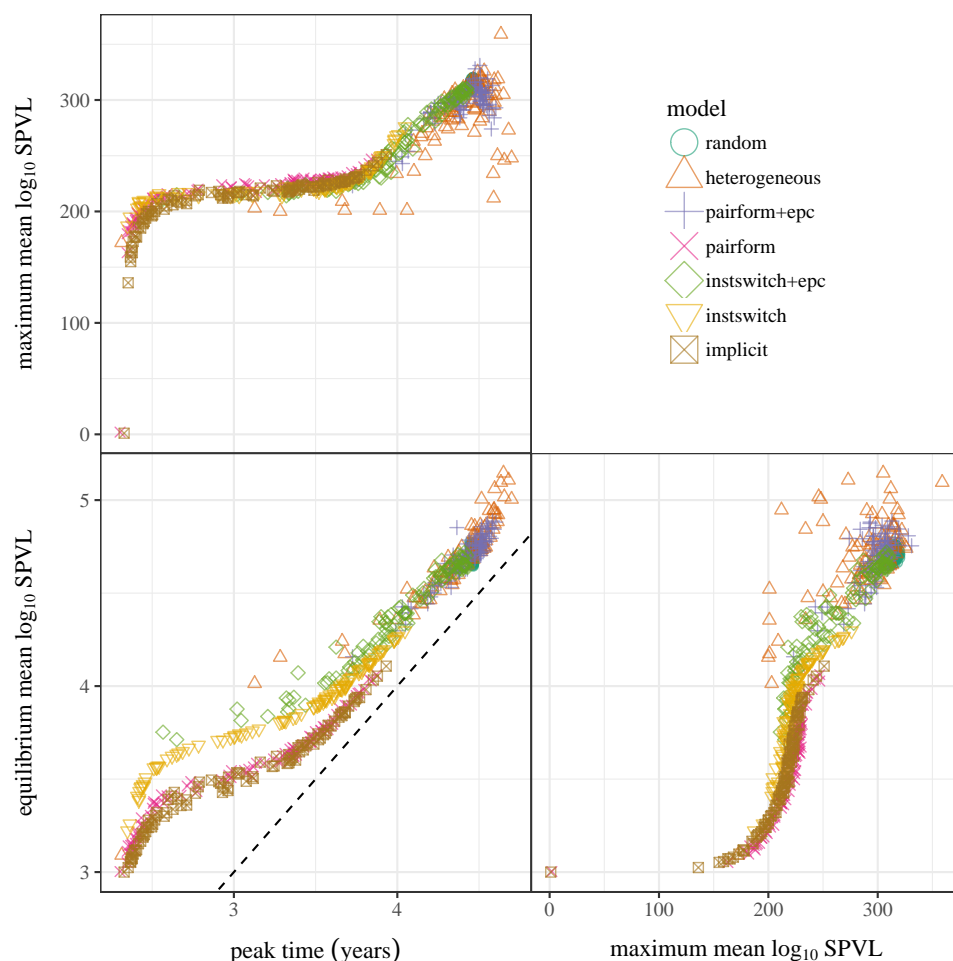
Fig 4. Pairs plot: bivariate relationships among summary statistics for each model structure. Three summary statistics obtained from each simulation have been plotted against each other to visualize the relationship among the summary statistics and to allow for clearer comparison between models. Surprisingly, the implicit model, an approximation for instantaneous partnership formation model (instswitch), shows an almost identical trend with a model that has pair formation dynamics (pairform). Dashed line in equilibrium vs. peak virulence plot shows 1:1 line, where equilibrium and peak virulence are equal. 100 values were sampled from each model to allow for clearer distinction between the models

transmission probability are even more extreme, about a fourfold difference: 0.249   336

(0.24-0.26), 0.252 (0.19-0.28), and 0.252 (0.15-0.28) per year for the random and   337

pairform+epc models vs. 0.059 (0.02-0.13) per year for the implicit model (see Appendix   338

S2 for plots showing univariate summaries of $\log_{10}$ SPVL and transmission probability).   339

The bivariate relationships (Fig 4) help distinguish the results of different models   340

with similar univariate dynamical summaries. While the relationship between   341
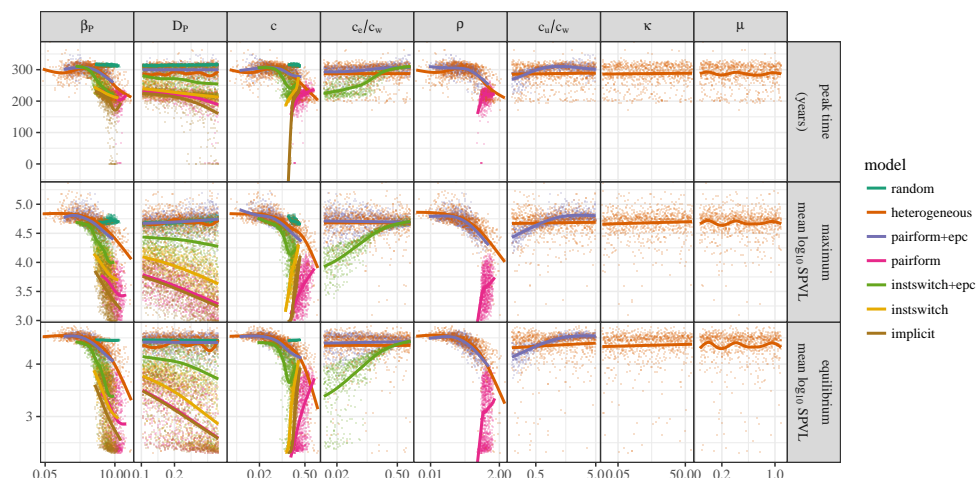
Fig 5. Sensitivity plot. For most parameters in the Latin hypercube samples, the figure shows the distribution (points) and trend (smooth line) of the summary statistic as a function of the parameter value, some of which have adjusted to achieve the standard initial epidemic growth rate (see Methods).
Opposing trends in summary statistics with respect to partnership dissolution rate, c, (third column) between the model with and without extra-pair contact illustrates that similar model with different assumptions may yield opposing predictions.

equilibrium progression time and peak time is similar for all model structures (top left panel), the other relationships show more variation. In particular, the implicit and pair-formation (without extra-pair contact) are very similar to each other, but distinct from the other models. We still do not have a convincing explanation for this distinction; we would have expected the implicit model to be most similar to the the instantaneous-switching model without extra-pair contact, which most closely matches its derivation. However, we note that the implicit model derivation is based on defining the force of infection to match a scaled version of $\mathcal{R}_0$, and as such would be expected to match the equilibrium behaviour but not necessarily the epidemic-phase behaviour of a model with explicit partnership dynamics.

Finally, the sensitivity plot (Fig 5) shows the effects of each parameter on the summary statistics. The most notable difference can be observed by comparing the scaled parameters (e.g. β_P, β_D, c, ρ) with the unscaled parameters (e.g. D_P, D_D, c_e/c_w, c_u/c_w, κ, μ); note that the effects of β_D and D_D are not shown in Fig 5 as their patterns are so similar to β_P and D_P, respectively.

One of the distinguishing features of the scaled parameters (in comparison to the unscaled parameters) is that the range of the parameters is compressed (relative to

other models) for models without extra-pair contact as those models require parameters to be scaled by a large value in order to achieve a given r of 0.04. Models with extra-pair contact show wide range parameters as they can display a wide range of dynamics depending on c_e/c_w (as well as c_u/c_w for models with uncoupled mixing) and thus require wide range of scaling factors to achieve the target r. Parameter range for random-mixing model is severely compressed because latin hypercube sampling does not affect the prevalence trajectory very much, and scaling factor does not vary much across parameters.

For parameters involved in partnership turnover (c and ρ), main distinction is between models with and without extra-pair contact. With extra-pair contact, we get gradual decrease in peak time, maximum $\log_{10}$ SPVL, and equilibrium $\log_{10}$ SPVL with increasing turnover rates; Otherwise we get increase in summary statistics. Although we have not verified this idea analytically, we speculate that increase in turnover rates diminishes the effect of epc (equivalently increasing relative importance of within-partnership contact), therefore selecting for lower $\log_{10}$ SPVL. For models without epc, increased rates of partnership change decrease the level of structured mixing (mimicing epc models), resulting in selection for higher $\log_{10}$ SPVL.

We also note that the implicit model and the instantaneous partnership formation model show similar patterns in scaled parameters. In fact, we can see that the effect of partnership dissolution rate, c, on equilibrium $\log_{10}$ SPVL of the two models are almost identical (in Fig 4, they have distinguishing features). Lastly, we note that increase in transmission rates (β_P and β_D) has a decreasing effect on summary statistics for all models except for random mixing model.

Surprisingly, once calibration is taken into account, the unscaled parameters have little to no effect overall. Increase in duration (D_P, D_D) in the primary and disease stages generally decrease the equilibrium virulence, peak virulence, and peak time, although the models with uncoupled mixing and random mixing model have high, relatively constant values with respect to these parameters. The ratio of extra-pair to within-pair contact (c_e/c_w) affects summary statistics in the instantaneous-switching +epc model, but not the pair-formation+epc model (probably because the uncoupled individuals present in the pair-formation+epc model make extra-pair contact by coupled individuals less important). Similarly, increasing the ratio of uncoupled to within-pair

contact, c_u/c_w, increases peak and equilibrium $\log_{10}$ SPVL and delays peak time of the pair-formation+epc model but has almost no effect on the heterogeneous model. Neither the uncoupled contact rate nor the mean (μ) or CV^2 of the number of non-cohabiting sexual partners has much systematic effect in the heterogeneous model.

Discussion

All models must simplify the world. Many constraints — among them data availability, computation time, and code complexity — drive the need for parsimony, with different constraints applying in different contexts. The critical question that modelers must ask is whether the simplified model gives adequate answers, or whether the simplifications lead to qualitative or quantitative errors. This question is especially important for modelers who are hoping that their conclusions will guide management decisions.

In the particular example of HIV virulence eco-evolutionary dynamics and the complexity of contact structures we reach the slightly ironic conclusion that the effort put into building a more realistic model essentially cancels out, putting us back where we started when used a naive random-mixing contact model. However, we are not quite back where we started, as the complex models lead to wider, presumably more realistic confidence intervals on the predictions. In general, unstructured mixing — whether occurring through purely random mixing, or through extra-pair contact and contact among people outside of stable partnerships — tends to drive faster virulence evolution, leading to higher peak virulence and lower times to progression at the peak time.

Taking further steps to make the model even more realistic might add further structure, making the random-mixing model predictions less accurate. For example, our model forms partnerships randomly, and assumes that extra-pair contact is randomly mixing across the population; one could instead model extra-pair contact as arising from multiple concurrent partnerships (some, such as contact with sex workers, of very short duration) and/or more structured partnership formation (by age, ethnicity, or behaviour group). The effects of other realistic complications such as explicit modeling of two sexes (both in contact structure and differential transmission probabilities), temporal and spatial variation in epidemic processes, or presence of genetic variation in hosts are harder to predict.

Parameterization is one of the biggest challenges of epidemiological modeling. In addition to following Champredon *et al.* [15] by doing Latin hypercube sampling across a wide range of epidemiological parameters, we calibrated each set of parameters to the same initial epidemic growth rate, chosen to match the results of previous models [10]. Previous models in this area have drawn their parameters from cohort studies from the 1990s [18, 26] rather than doing any explicit calibration to epidemic curves, but they give reasonable order-of-magnitude growth rates (≈ 0.04 year^{-1}) for the early stages of the HIV epidemic (although considerably lower than estimates of $\approx 0.07 - 0.1$ year^{-1} based on population genetic reconstructions [27]). However, our reason for calibrating was not to match any specific observed epidemic, but rather to make sure that we were making meaningful comparisons across a range of models with radically different contact structures, and hence involving different interpretations of the same quantitative parameters. For example, in models with instantaneous switching the partnership dissolution rate c is identical to the partnership formation rate; in models with explicit partnership formation, the partnership formation rate is also c at equilibrium, but might vary over the course of an epidemic. It is not obvious whether models with equal parameters but different structures should be directly compared; calibration solves this problem.

More generally, any model that wants to be taken seriously for management and forecasting purposes should be calibrated to *all* available data, using informative priors to incorporate both realistic distributions of uncertainty for all parameters from independent measurements [28] and calibration from population-level observations of epidemic trajectories. Such a procedure would also be an improvement on the common — although not universal — practice, which we have followed here, of assessing uncertainty over uniform ranges rather than using distributions that allow more continuous variation in support over the range of a parameter.

Researchers have documented that HIV virulence and set-point viral load are changing, on time scales comparable to those portrayed here (e.g., compare Fig 2 to Herbeck *et al.*'s estimated rate of change of 1.3 log$_{10}$ SPVL per century [95% CI -0.1 to 3] [29]), and have begun to build relatively realistic models that attempt to describe how interventions such as mass antiretroviral therapy (ART) can be expected to change the trajectory of virulence evolution [12, 30, 31]. While these efforts are well-intentioned,

we caution that structural details that are currently omitted from these models could   453
significantly change their conclusions.   454

Acknowledgements   455

Supporting Information   460

Appendix S1: Model Details   461

Appendix S2: Dynamics of Transmission and Virulence   462

References

1. Alizon S, Hurford A, Mideo N, van Baalen M. Virulence evolution and the trade-off hypothesis: history, current state of affairs and the future. J Evol Biol. 2009;22:245–259. doi:10.1111/j.1420-9101.2008.01658.x.

2. Ebert D, Bull JJ. Challenging the trade-off model for the evolution of virulence: is virulence management feasible? Trends Microbiol. 2003;11(1):15–20.

3. Alizon S, Michalakis Y. Adaptive virulence evolution: the good old fitness-based approach. Trends in Ecology & Evolution. 2015;30(5):248–254. doi:10.1016/j.tree.2015.02.009.

4. Dwyer G, Levin SA, Buttel L. A simulation model of the population dynamics and evolution of myxomatosis. Ecol Monog. 1990;60:423–447.

5. Mackinnon MJ, Read AF. Genetic relationships between parasite virulence and transmission in the rodent malaria *Plasmodium chabaudi*. Evolution. 1999; p. 689–703.

6. Jensen KH, Little T, Skorping A, Ebert D. Empirical support for optimal virulence in a castrating parasite. PLoS Biol. 2006;4(7):e197.

7. De Roode JC, Yates AJ, Altizer S. Virulence-transmission trade-offs and population divergence in virulence in a naturally occurring butterfly parasite. Proceedings of the National Academy of Sciences. 2008;105(21):7489–7494.

8. Fraser C, Hollingsworth TD, Chapman R, de Wolf F, Hanage WP. Variation in HIV-1 set-point viral load: Epidemiological analysis and an evolutionary hypothesis. PNAS. 2007;104:17441–17446.

9. Fraser C, Lythgoe K, Leventhal GE, Shirreff G, Hollingsworth TD, Alizon S, et al. Virulence and Pathogenesis of HIV-1 Infection: An Evolutionary Perspective. Science. 2014;343(6177):1243727. doi:10.1126/science.1243727.

10. Shirreff G, Pellis L, Laeyendecker O, Fraser C. Transmission Selects for HIV-1 Strains of Intermediate Virulence: A Modelling Approach. PLoS Computational Biology. 2011;7(10):e1002185. doi:10.1371/journal.pcbi.1002185.

11. Herbeck JT, Mittler JE, Gottlieb GS, Mullins JI. An HIV Epidemic Model Based on Viral Load Dynamics: Value in Assessing Empirical Trends in HIV Virulence and Community Viral Load. PLoS Comput Biol. 2014;10(6):e1003673.

12. Herbeck JT, Mittler JE, Gottlieb GS, Goodreau SM, Murphy JT, Cori A, et al. Evolution of HIV virulence in response to widespread scale up of antiretroviral therapy: a modeling study. Virus Evolution. 2016;2(2):vew028. doi:10.1093/ve/vew028.

13. Day T, Proulx SR. A General Theory for the Evolutionary Dynamics of Virulence. The American Naturalist. 2004;163(4):E40–E63. doi:10.1086/382548.

14. Alizon S. The Price equation framework to study disease within-host evolution. Journal of Evolutionary Biology. 2009;22(5):1123–1132. doi:10.1111/j.1420-9101.2009.01726.x.

15. Champredon D, Bellan S, Dushoff J. HIV Sexual Transmission Is Predominantly Driven by Single Individuals Rather than Discordant Couples: A Model-Based Approach. PLoS ONE. 2013;8(12):e82906. doi:10.1371/journal.pone.0082906.

16. Dietz K, Hadeler KP. Epidemiological models for sexually transmitted diseases. Journal of Mathematical Biology. 1988;26(1):1–25.

17. Kretzschmar M, Dietz K. The effect of pair formation and variable infectivity on the spread of an infection without recovery. Mathematical Biosciences. 1998;148(1):83–113.

18. Hollingsworth TD, Anderson RM, Fraser C. HIV-1 Transmission, by Stage of Infection. Journal of Infectious Diseases. 2008;198(5):687–693. doi:10.1086/590501.

19. Omori R, Chemaitelly H, Abu-Raddad LJ. Dynamics of non-cohabiting sex partnering in sub-Saharan Africa: a modelling study with implications for HIV transmission. Sexually Transmitted Infections. 2015;doi:10.1136/sextrans-2014-051925.

20. May RM, Anderson RM. The Transmission Dynamics of Human Immunodeficiency Virus (HIV). Philosophical Transactions of the Royal Society of London Series B, Biological Sciences. 1988;321(1207):565–607.

21. Delva W, Leventhal GE, Helleringer S. Connecting the dots: network data and models in HIV epidemiology. AIDS. 2016;30(13):2009–2020. doi:10.1097/QAD.0000000000001184.

22. Blower SM, Hartel D, Dowlatabadi H, Anderson RM, May RM. Drugs, Sex and HIV: A Mathematical Model for New York City. Philosophical Transactions of the Royal Society of London B: Biological Sciences. 1991;331(1260):171–187. doi:10.1098/rstb.1991.0006.

23. Ma J, Dushoff J, Bolker BM, Earn DJD. Estimating Initial Epidemic Growth Rates. Bulletin of Mathematical Biology. 2014;76(1):245–260. doi:10.1007/s11538-013-9918-2.

24. Wallinga J, Lipsitch M. How generation intervals shape the relationship between growth rates and reproductive numbers. Proceedings of the Royal Society of London B: Biological Sciences. 2007;274(1609):599–604. doi:10.1098/rspb.2006.3754.

25. Soetaert K, Petzoldt T, Setzer RW. Solving Differential Equations in R: Package deSolve. Journal of Statistical Software. 2010;33(9):1–25. doi:10.18637/jss.v033.i09.

26. Wawer MJ, Gray RH, Sewankambo NK, Serwadda D, Li X, Laeyendecker O, et al. Rates of HIV-1 transmission per coital act, by stage of HIV-1 infection, in Rakai, Uganda. Journal of Infectious Diseases. 2005;191(9):1403–1409.

27. Faria NR, Rambaut A, Suchard MA, Baele G, Bedford T, Ward MJ, et al. The early spread and epidemic ignition of HIV-1 in human populations. Science (New York, NY). 2014;346(6205):56–61. doi:10.1126/science.1256739.

28. Elderd BD, Dukic VM, Dwyer G. Uncertainty in predictions of disease spread and public health responses to bioterrorism and emerging diseases. Proceedings

of the National Academy of Sciences. 2006;103(42):15693 –15697.
doi:10.1073/pnas.0600816103.

29. Herbeck JT, Müller V, Maust BS, Ledergerber B, Torti C, Di Giambenedetto S,
et al. Is the virulence of HIV changing? A meta-analysis of trends in prognostic
markers of HIV disease progression and transmission. AIDS (London, England).
2012;26(2):193–205. doi:10.1097/QAD.0b013e32834db418.

30. Payne R, Muenchhoff M, Mann J, Roberts HE, Matthews P, Adland E, et al.
Impact of HLA-driven HIV adaptation on virulence in populations of high HIV
seroprevalence. Proceedings of the National Academy of Sciences.
2014;111(50):E5393–E5400. doi:10.1073/pnas.1413339111.

31. Roberts HE, Goulder PJ, McLean AR. The impact of antiretroviral therapy on
population-level virulence evolution of HIV-1. Journal of The Royal Society
Interface. 2015;12(113):20150888.